

EurJIC

European Journal of Inorganic Chemistry

 **Chemistry
Europe**

European Chemical
Societies Publishing

Accepted Article

Title: Synthetic Approaches to and Structures of Diplatinum Polyynediyl Complexes $\text{trans,trans-}[(\text{C}_6\text{F}_5)(\text{R}_3\text{P})_2\text{Pt}(\text{C}\equiv\text{C})_n\text{Pt}(\text{PR}_3)_2(\text{C}_6\text{F}_5)]$ With Odd Numbers of Triple Bonds; Avoiding Complicating Ethynediyl Extrusions

Authors: SOURAJIT DEY BAKSI, Nancy Weisbach, Nattamai Bhuvanesh, and John A. Gladysz

This manuscript has been accepted after peer review and appears as an Accepted Article online prior to editing, proofing, and formal publication of the final Version of Record (VoR). The VoR will be published online in Early View as soon as possible and may be different to this Accepted Article as a result of editing. Readers should obtain the VoR from the journal website shown below when it is published to ensure accuracy of information. The authors are responsible for the content of this Accepted Article.

To be cited as: *Eur. J. Inorg. Chem.* **2024**, e202400428


Link to VoR: <https://doi.org/10.1002/ejic.202400428>

Synthetic Approaches to and Structures of Diplatinum Polyynediyl Complexes
trans,trans-[(C₆F₅)(R₃P)₂Pt(C≡C)_nPt(PR₃)₂(C₆F₅)] With Odd Numbers of Triple
Bonds; Avoiding Complicating Ethynediyl Extrusions

Sourajit Dey Baksi,^[a] Nancy Weisbach,^[a] Nattamai Bhuvanesh,^[a] and John A. Gladysz*^[a]

ABSTRACT: Reactions of *trans*-(C₆F₅)(*p*-tol₃P)₂Pt(C≡C)_nSiEt₃ (**PtC_{2n}Si**; *n* = 5, 7, 9) and excess **PtCl** in the presence of wet *n*-Bu₄N⁺ F⁻ (to effect protodesilylation) under Sonogashira-type conditions (CuCl, base, other additives) afford the title compounds **PtC₁₀Pt**, **PtC₁₄Pt**, and **PtC₁₈Pt** in 42-32% yields. A four-fold substitution of the phosphine ligands in **PtC₁₀Pt** by PEt₃ affords **Pt'C₁₀Pt'** (78%), and a Sonogashira reaction of **Pt'C₂H** and **Pt'Cl** affords **Pt'C₂Pt'** (68%). The analogous reaction with **PtC₂Si** and **PtCl** is unsuccessful, presumably for steric reasons. The crystal structures of **PtC₁₀Pt**, **PtC₁₄Pt**, **Pt'C₁₀Pt'**, and **Pt'C₂Pt'** exhibit a number of interesting trends and features. Certain *sp* chain extension reactions that lead to or employ the precursors **PtC₁₀Si**, **PtC₁₂Si**, **PtC₁₄Si**, and **PtC₁₈Si** sometimes give byproducts derived from C₂ loss, and possible origins are discussed. Related phenomena have been reported by others in the course of synthesizing extended conjugated polyynes.

[a] Mr. S. Dey Baksi, Dr. N. Weisbach, Dr. N. Bhuvanesh, Prof. J. A. Gladysz
Department of Chemistry, Texas A&M University
P.O. Box 30012
College Station, Texas, 77842-3012, USA
E-mail: gladysz@mail.chem.tamu.edu
<https://www.chem.tamu.edu/rgroup/gladysz/index.html>

 Supporting information for this article is available on the WWW under <https://doi.org/10.1002/ejic.202200xxxx>

submitted to *Eur. J. Inorg. Chem.* for the special collection on
"Emerging Trends in Organometallics and Catalysis"

■ INTRODUCTION

As illustrated in Figure 1, very long conjugated polyynes, endgroup-(C≡C)_n-endgroup, are now isolable with 24-26 triple bonds, representing C₄₈-C₅₂ linkages.^[1-4] These efforts have been prompted by (1) an interest in modeling the properties of the sp hybridized carbon allotrope, carbyne,^[5] which is believed to have the polyyne structure -(C≡C)-_∞, and (2) the sport in creating new forms of carbon,^[6] fueled in part by materials applications and attention in popular media.^[7] However, most synthetic approaches to such polyynes entail the stepwise extension of the (C≡C)_n chains, as exemplified in Scheme 1 (bottom), and culminate in homocoupling reactions that double the number of triple bonds to 2n. Hence, there is a methodological bias favoring even numbers of C≡C linkages.

However, to best model carbyne, many properties must be quantified as a function of sp chain length. Thus, representatives with odd numbers of triple bonds have been essential for thorough analyses. Also, in C≡C reactivity studies, polyynes with even numbers of triple bonds will by necessity give 1:1 adducts that are unsymmetrical. In contrast, with polyynes with odd numbers of triple bonds, there is the potential for symmetrical 1:1 adducts, such in additions of species with mirror planes (A-A).^[8] As the sp chains are extended, the inner C≡C linkages are distanced from the frequently bulky endgroups and become sterically more accessible.

Our previous studies of polyynes have made extensive use of the platinum endgroup *trans*-(C₆F₅)(*p*-tol₃P)₂Pt (**Pt**).^[3,9] Specifically, we have reported the synthesis and isolation of diplatinum polyynediyl complexes *trans,trans*-[(C₆F₅)(*p*-tol₃P)₂Pt(C≡C)_nPt(*p*-tol₃)₂(C₆F₅)] (**PtC_{2n}Pt**) where *n* includes the even numbers 2, 4, 6, 8, 10, 12, 14, 16, 18, 20, 22, 24, and 26 (**PtC₄Pt**, **PtC₈Pt**, **PtC₁₂Pt**, **PtC₁₆Pt**, **PtC₂₀Pt**, **PtC₂₄Pt**, **PtC₂₈Pt**, **PtC₃₂Pt**, **PtC₃₆Pt**, **PtC₄₀Pt**, **PtC₄₄Pt**, **PtC₄₈Pt**, and **PtC₅₂Pt** in Figure 1). However, only a single complex of this type has heretofore been prepared with an odd number of triple bonds, **PtC₆Pt**.^[9a,10] It was synthesized as shown in Scheme 1 (top) by what can be viewed as a Sonogashira-like coupling^[11] of **PtC₆H**^[9a] and **Pt-Cl**^[9a] (cat. CuCl, Et₂NH cosolvent that neutralizes the HCl evolved). As illustrated below, the triarylphosphine ligands significantly sterically shield the central C≡C linkage.

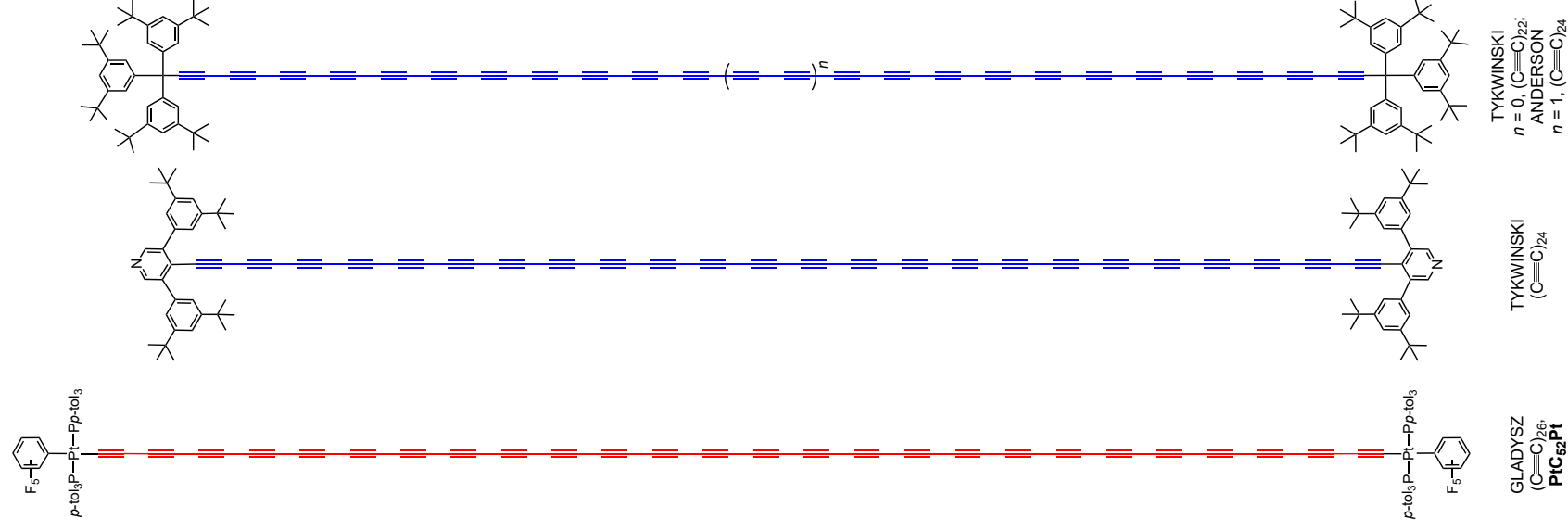
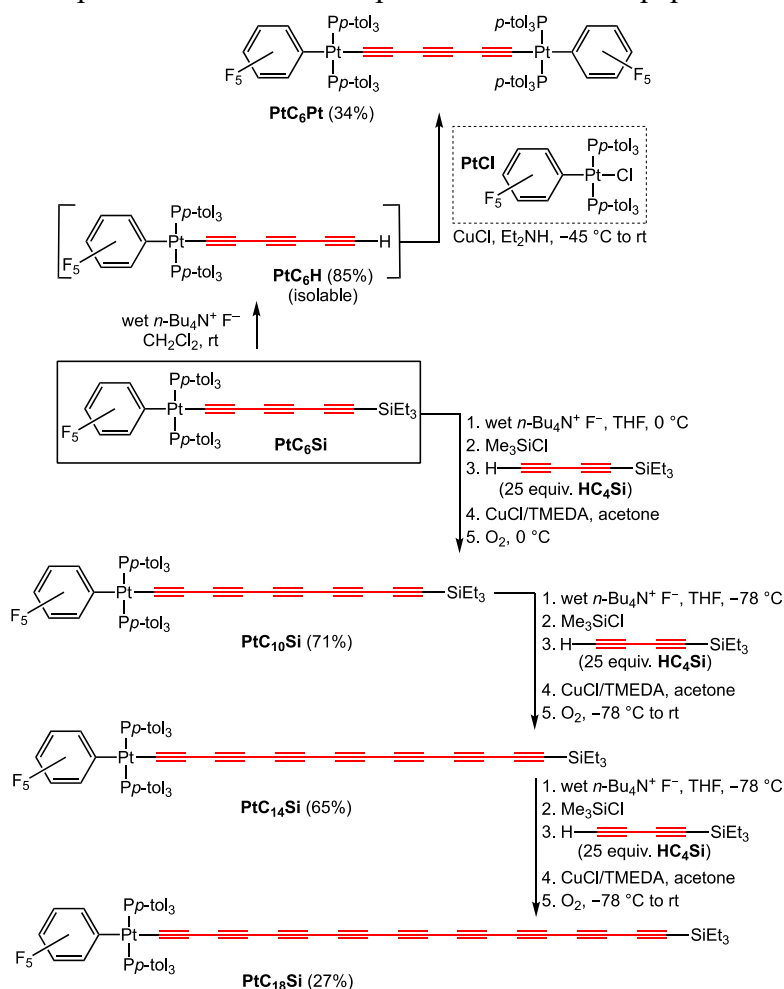


Figure 1. The longest polyynes that are currently isolable.

Accordingly, in this paper we report expedient syntheses of the corresponding polyynediyl complexes with $n = 5, 7,$ and 9 . The published routes to the necessary starting materials are summarized in Scheme 1,^[9a,12] and become important in other contexts below. With $n = 5$, four-fold phosphine substitution to give the PtEt_3 analog ($\text{Pt}'\text{C}_{10}\text{Pt}'$) is also described, and for the sake of completeness approaches to the lowest homologs PtC_2Pt and $\text{Pt}'\text{C}_2\text{Pt}'$ ($n = 1$) are explored. Most of these complexes are structurally characterized. No portion of this work has been communicated, although to avoid fragmentary treatments snippets of spectroscopic data for PtC_{10}Pt , PtC_{14}Pt , and PtC_{18}Pt were incorporated into tables and plots in a recent full paper describing PtC_{52}Pt .^[3]

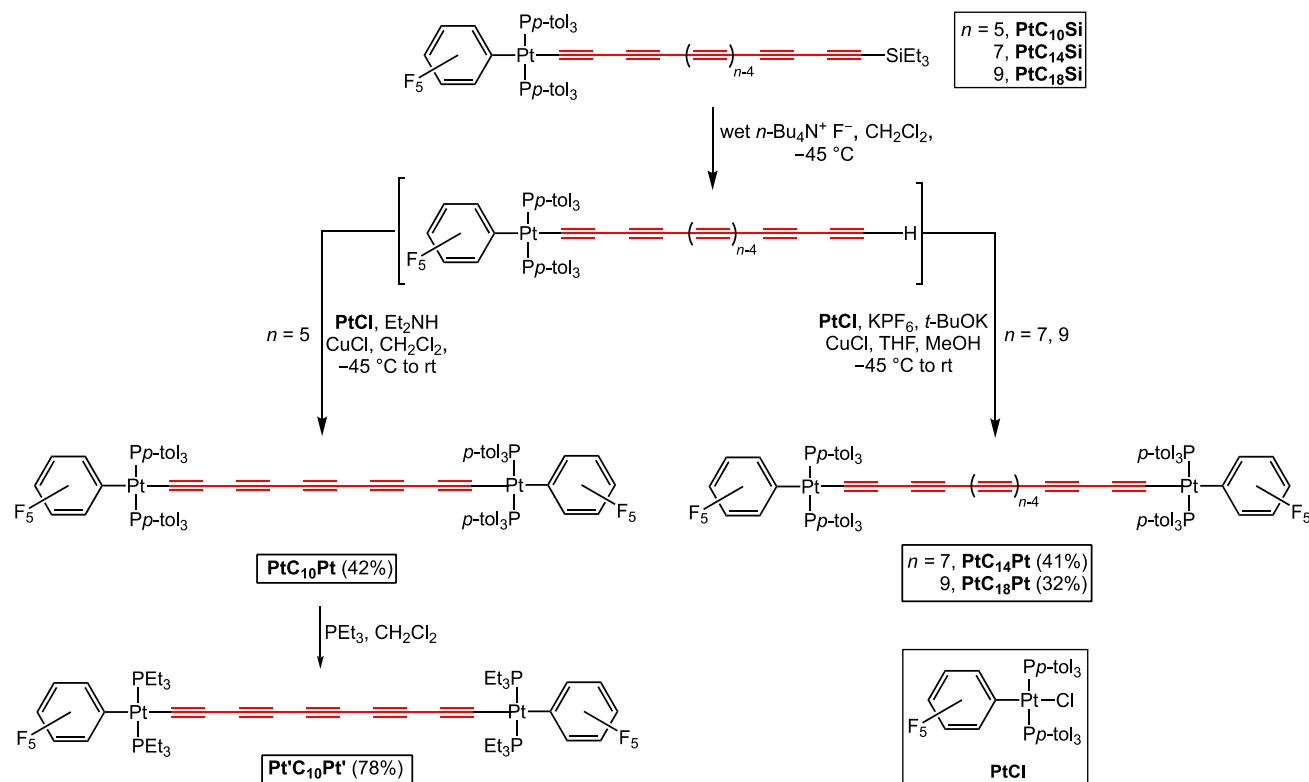


■ RESULTS

1. Syntheses. The chloride complex PtCl and terminal polyynyl complexes PtC_xH are required for Sonogashira-like syntheses of PtC_xPt . The building blocks PtC_4H ,^[9a] PtC_6H ,^[9a]

and PtC_8H ^[9c] can be isolated, but become progressively less stable. Higher homologs, at least through $n = 9$ or PtC_{18}H , can be generated from PtC_xSi ($\text{Si} = \text{SiEt}_3$) by treatment with wet $n\text{-Bu}_4\text{N}^+ \text{F}^-$ at low temperature, as inferred by TLC and/or trapping via click azide cycloadditions.^[12] Such protodesilylations are involved in every step in Scheme 1 above, and the *in situ* methodology is often used for the isolable but still sensitive educts PtC_6H and PtC_8H .

As shown in Scheme 2, PtC_{10}Si and wet $n\text{-Bu}_4\text{N}^+ \text{F}^-$ were combined in CH_2Cl_2 at -45°C to generate PtC_{10}H . In a separate flask, PtCl (1.1 equiv), CuCl (0.9 equiv), and excess Et_2NH were combined in CH_2Cl_2 at -45°C . The former solution was added to the latter. A chromatographic workup gave the target complex PtC_{10}Pt as an air stable yellow powder in 42% yield. However, analogous procedures with PtC_{14}Si and PtC_{18}Si gave very poor yields of the corresponding adducts PtC_{14}Pt and PtC_{18}Pt .



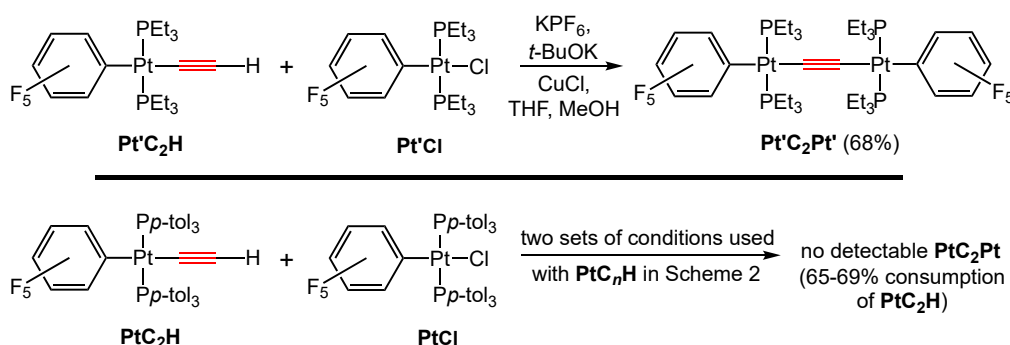
Scheme 2. Syntheses of title complexes.

Another literature recipe for the coupling of metal halides and terminal organic alkynes utilizes $t\text{-BuOK}$, KPF_6 , and MeOH , either with or without CuCl .^[13,14] Accordingly, the CH_2Cl_2 solutions derived from PtC_{14}Si or PtC_{18}Si and wet $n\text{-Bu}_4\text{N}^+ \text{F}^-$ were added to THF/MeOH solu-

tions of PtCl , CuCl , $t\text{-BuOK}$, and KPF_6 . Workups gave PtC_{14}Pt or PtC_{18}Pt as dark yellow powders in 41-32% yields. An analogous reaction with PtC_{22}Si ^[3] did not give detectable amounts of the desired PtC_{22}Pt .

For certain reactivity studies, sterically less encumbered platinum endgroups were sought. It has been previously established that triarylphosphine ligands of diplatinum polyynediyl complexes can be thermally replaced by trialkylphosphine ligands.^[9a,10] Thus, as shown in Scheme 2, PtC_{10}Pt and PEt_3 (4.6 equiv) were combined in CH_2Cl_2 . After 16 h, workup gave $\text{Pt}'\text{C}_{10}\text{Pt}'$ as an air stable yellow powder in 78% yield. The complexes $\text{Pt}'\text{C}_6\text{Pt}'$,^[10] $\text{Pt}'\text{C}_8\text{Pt}'$,^[9a] and $\text{Pt}'\text{C}_{12}\text{Pt}'$ ^[9a] have been similarly synthesized.

Finally, we sought the lowest homolog in this series of compounds with an odd number of triple bonds, PtC_2Pt . Other complexes with PtC_2Pt linkages have been of interest in our group due to possibilities (with appropriate substitution) for atropisomerism.^[15] However, when PtC_2H ^[16] and PtCl were combined under either of the heterocoupling conditions in Scheme 2, the PtC_2H was slowly consumed but most PtCl remained (Scheme 3). Next, the less bulky building blocks $\text{Pt}'\text{C}_2\text{H}$ ^[16] and $\text{Pt}'\text{Cl}$ ^[16] were combined in the presence of KPF_6 , $t\text{-BuOK}$, and CuCl . After 2 d, $\text{Pt}'\text{C}_2\text{Pt}'$ could be isolated as a white solid in 68% yield.



Scheme 3. Routes to $\text{Pt}'\text{C}_2\text{Pt}'$ and PtC_2Pt investigated.

All new complexes were characterized by microanalyses and NMR (^1H , $^{13}\text{C}\{^1\text{H}\}$, $^{31}\text{P}\{^1\text{H}\}$, $^{19}\text{F}\{^1\text{H}\}$) and IR spectroscopy, as summarized in the experimental section. UV-visible spectra were recorded except for $\text{Pt}'\text{C}_2\text{Pt}'$, and those of PtC_{10}Pt , PtC_{14}Pt , and PtC_{18}Pt are depicted in Figure 2, together with that of previously reported PtC_{20}Pt .^[9b] The $^{13}\text{C}\{^1\text{H}\}$ NMR, $^{31}\text{P}\{^1\text{H}\}$ NMR, and UV-visible spectra exhibit a number of trends that have been carefully interpreted in a

recent full paper dealing with PtC_{52}Pt .^[3] Readers are referred to that work for details.

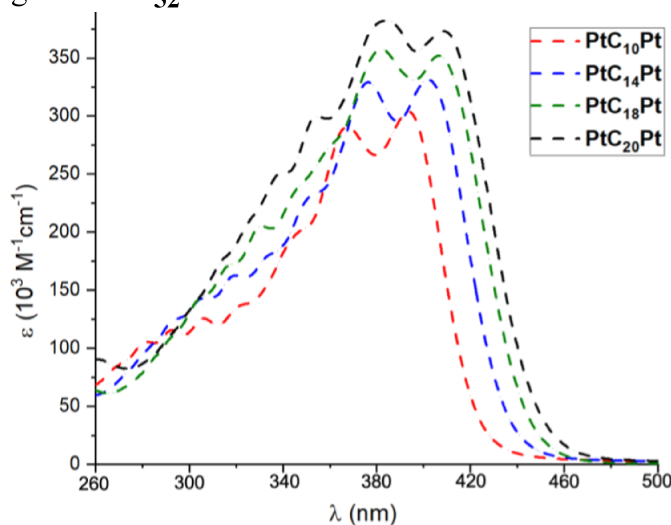


Figure 2. UV-visible spectra of PtC_xPt (2.25×10^{-6} M in CH_2Cl_2).

2. Crystallography. Diplatinum complexes in this series are frequently crystalline, and single crystals of PtC_{10}Pt , PtC_{14}Pt , $\text{Pt}'\text{C}_{10}\text{Pt}'$, and $\text{Pt}'\text{C}_2\text{Pt}'$ could be grown as described in the experimental section. The first was obtained as a chloroform disolvate. Their structures were solved as outlined in Table s1 and the experimental section. Thermal ellipsoid diagrams are given in Figure 3, with the first two complexes showing the usual $\text{C}_6\text{H}_4\text{CH}_3/\text{C}_6\text{F}_5/\text{C}_6\text{H}_4\text{CH}_3$ π stacking interactions.^[17] Key metrical parameters are summarized in Table s2, all of which compare closely to other structurally characterized $\text{Pt}(\text{C}\equiv\text{C})_n\text{Pt}$ species.^[3,9,12,18] The molecular structure of PtC_{10}Pt exhibited a C_2 axis and that of $\text{Pt}'\text{C}_{10}\text{Pt}'$ an inversion center. In both cases, this exchanged the two PtC_5 segments and ligands on opposite termini.

3. Side reactions involving ethynediyl (C_2) extrusion. Throughout the synthetic studies leading to molecules of the types in Figure 1, including lower homologs with different endgroups, researchers have sometimes noted unexpected byproducts in coupling and cross-coupling reactions derived from the loss of C_2 .^[1,9a,19] Our citation list is thought to be complete, but the details are often cached in the SI or as footnotes. Sometimes greater numbers of carbon atoms are lost, which are always even.^[19a,20] It remains unclear as to whether these represent consecutive losses of C_2 or higher C_x species. There is also the question of whether such byproducts are derived from small amounts of lower polyynes nefariously lurking in the precursors.

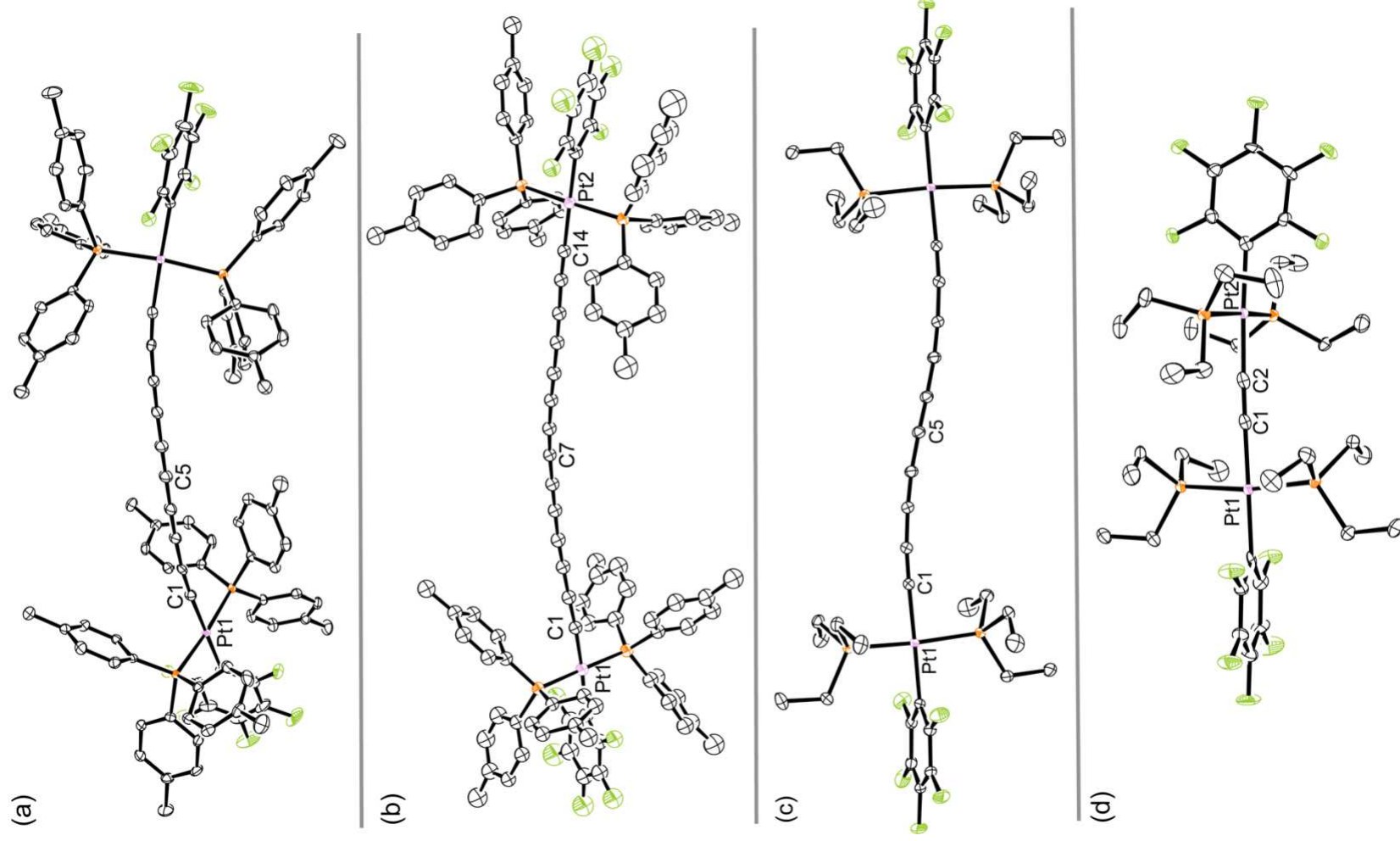
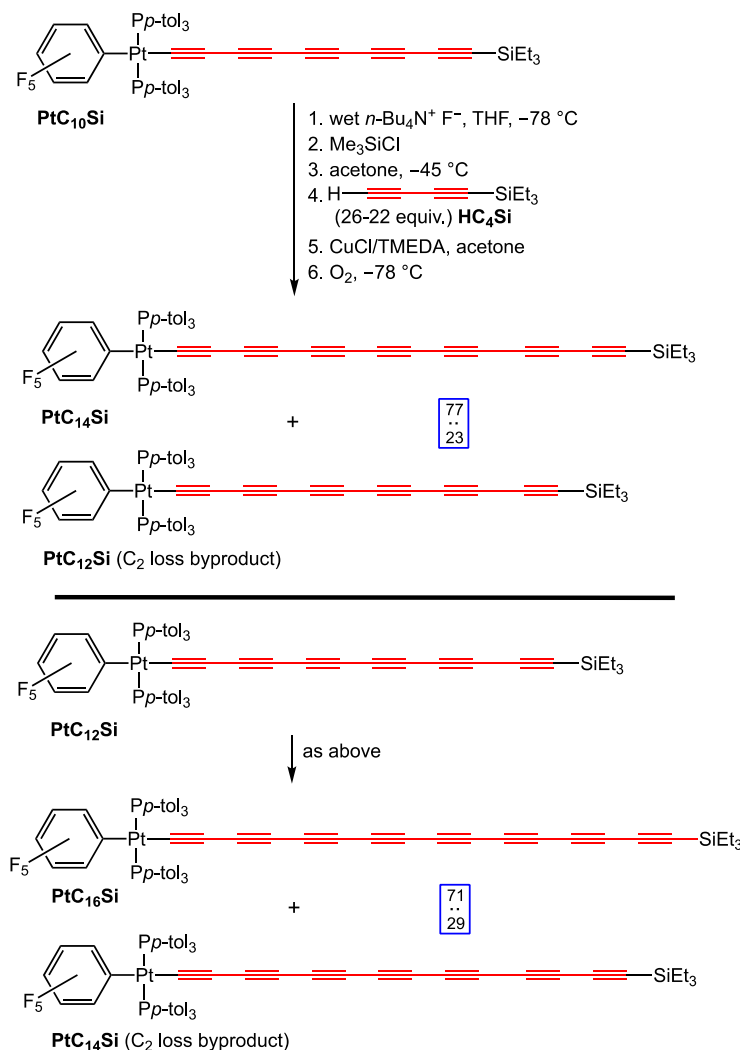


Figure 3. Thermal ellipsoid plots (50% probability level) for (a) $\text{PtC}_{10}\text{Pt}(\text{CHCl}_3)_2$, (b) PtC_{14}Pt , (c) $\text{Pt}'\text{C}_{10}\text{Pt}'$, and (d) $\text{Pt}'\text{C}_2\text{Pt}'$ with hydrogen atoms and solvent molecules omitted. For metrical parameters, see Table S2.

The protocols provided in our synthesis of PtC_{52}Pt ^[3] avoid this bothersome issue, but it remains important to check samples of PtC_xSi and HC_xSi for homogeneity by ^{13}C NMR as they are synthesized. A signal/noise level similar to that for PtC_{12}Si in Figure 4-A should be sought. The problem seems to occur more frequently when Hay oxidative cross couplings, three examples of which are given in Scheme 1 (CuCl/TMEDA , acetone, O_2 , excess HC_4Si),^[21] are conducted under certain conditions. Complications with Hay oxidative *homocouplings* have been rare. Thus, this full paper is used as a vehicle for reporting some well documented ethynediyl extrusions involving the building blocks in Schemes 1 and 2 but different reaction conditions. These experiments were conducted contemporaneously with the same sources of chemicals (e.g., CuCl , solvent purification, etc.).



Scheme 4. Oxidative heterocoupling reactions of PtC_{10}Si and PtC_{12}Si that give byproducts derived from C_2 loss.

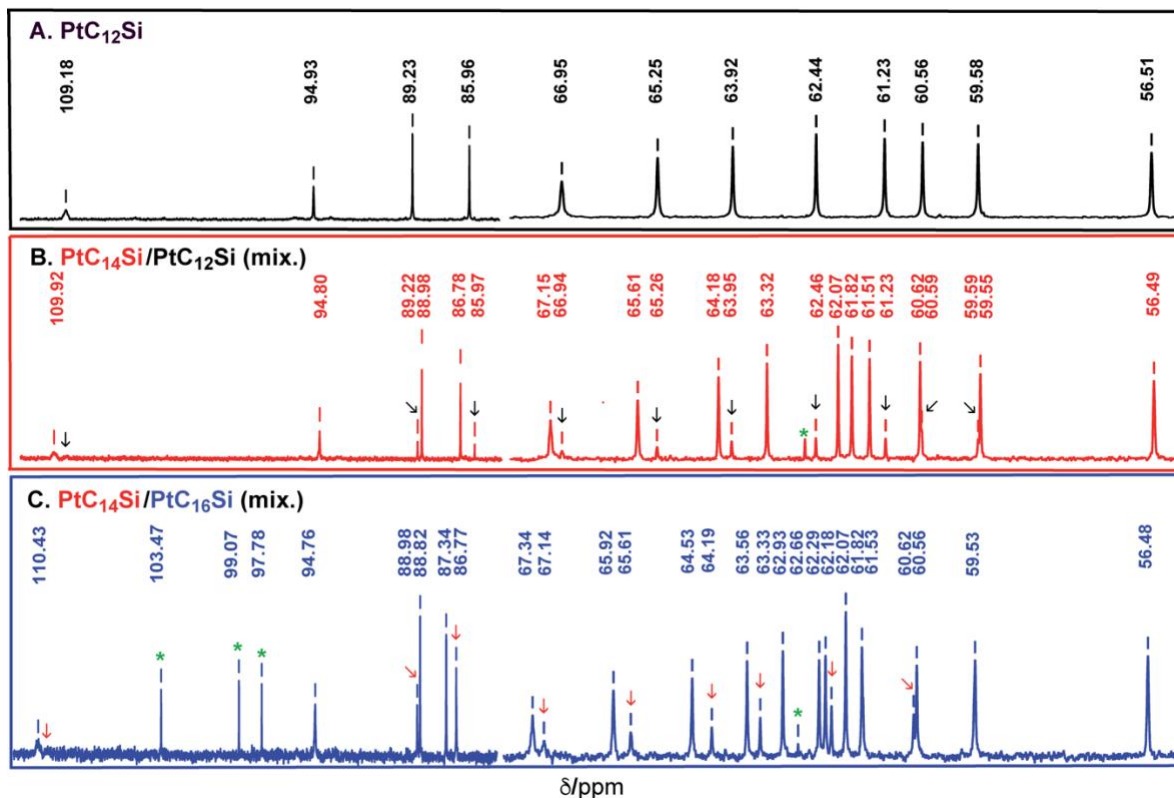


Figure 4. Partial $^{13}\text{C}\{^1\text{H}\}$ NMR spectra (CDCl₃, sp region) of pure PtC₁₂Si (top panel, A, black), and the PtC₁₄Si/PtC₁₂Si (middle panel, B, red; black arrows indicate the PtC₁₂Si signals), and PtC₁₄Si/PtC₁₆Si mixtures (bottom panel, C, blue; red arrows indicate the PtC₁₄Si signals) generated in Scheme 4. Asterisks (*) denote impurity signals, and the solvent peak (77.0 ppm) has been excised.

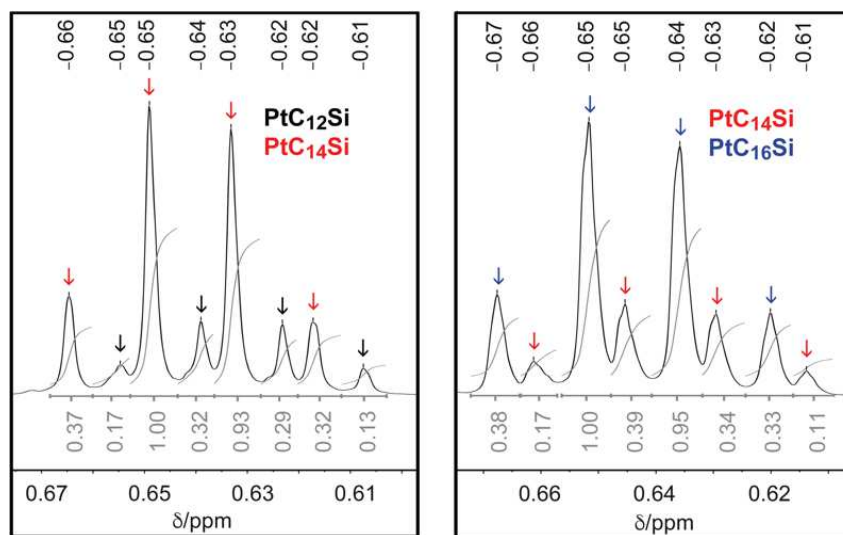


Figure 5. The SiCH₂ ^1H NMR signals (CDCl₃) of the PtC₁₄Si/PtC₁₂Si (left) and PtC₁₆Si/PtC₁₄Si (right) mixtures generated in Scheme 4. The integrations used to assign the 77:23 and 71:29 ratios are depicted.

As depicted in Scheme 4, PtC₁₀Si^[12] and PtC₁₂Si^[12] were protodesilylated to PtC₁₀H and PtC₁₂H at -78°C using our standard conditions, followed by cross coupling with ca. 25 equivalents of HC₄Si^[12] under Hay conditions. Such stoichiometries, intended in this case to maxim-

ize the ratio of platinum cross- versus homocoupling, are typical in polyene syntheses. Workups gave samples of **PtC₁₄Si** and **PtC₁₆Si**, but careful attention to the ¹³C{¹H} NMR spectra (Figures 4-B,C) showed that they were actually **PtC₁₄Si/PtC₁₂Si** and **PtC₁₆Si/PtC₁₄Si** mixtures (43 and 25% total yields, respectively).^[22] This was also evident from the SiCH₂ ¹H NMR signals, illustrated in Figure 5. Despite some peak overlap, analyses indicated 77:23 and 71:29 ratios. However, all attempts to separate the components by analytical or preparative HPLC were unsuccessful.^[23]

The preceding phenomena were noted with two different batches of **HC₄Si**. Also, given the large excesses used, only traces of **HC₂Si** would be required to account for the C₂ loss products in Scheme 4. However, oxidative heterocouplings of **HC₄Si** are much faster than those of **HC₂Si**,^[24] paralleling trends well documented for **PtC_xH**.^[3,9a] A reaction of **PtC₁₀Si** analogous to that in Scheme 4 was also carried out with tri(isopropyl)silyl (TIPS) butadiyne, **HC₄Si**.^[12] As detailed in the SI, a 53:47 **PtC₁₄Si'/PtC₁₂Si'** mixture was obtained (39% total yield). In our most recent work,^[3] where ethynediyl loss has not been a factor, care has been taken to slowly add the blue Hay catalyst supernatant (avoiding addition of the light green precipitate), and omit the acetone addition step (compare step 3 in Schemes 1 and 4).

■ DISCUSSION

This study has extended the Sonogashira protocol for the synthesis of complexes with Pt-(C≡C)_nPt linkages to a wider range of species with odd numbers of triple bonds (*n*). In the series **PtC_xPt**, adducts with *n* = 3 through *n* = 9 are now available, although the prospects for higher homologs are uncertain, given that **PtC₂₂Si** could not be successfully applied in Scheme 2. This presumably reflects the stage at which the rate of **PtC_xH** decomposition becomes faster than the rate of reaction with **PtCl**, a type of limit reached in most derivatizations of **PtC_xH**.

Although steric issues appear to preclude access to **PtC₂Pt**, when the phosphine ligands are downsized to PEt₃, **Pt'C₂Pt'** becomes available. Interestingly, when *one* *p*-tol₃P ligand on each terminus of **PtC₂Pt** is replaced by the smaller phosphine PhMe₂P, a Sonogashira synthesis becomes feasible.^[15] However, the *p*-tol₃P and PhMe₂P ligands statistically scramble, affording a multitude of products. Presumably, *p*-tol₃P exchange also occurs in Schemes 2 and 3, but is not

detectable in the absence of deuterium or similar labeling.

There are several other strategies for preparing conjugated polyynes with odd numbers of triple bonds. An obvious example is the Fritsch-Buttenberg-Wiechell rearrangement^[25] of carbenes or carbenoids of the type $(R(C\equiv C)_n)_2C=C:$.^[4a,19b-d] Tykwinski has applied this to the synthesis of pentaynes^[19b] (and in two-fold variants, higher polyynes^[19b,d]). Also, the diiodo building blocks $I(C\equiv C)_nI$ are available with $n = 1, 3,$ and 5 . These have been combined in various coupling recipes to prepare a number of symmetrically substituted pentaynes and heptaynes.^[26] Triynes and pentaynes have also been systematically constructed from 3-cyclobutene-1,2-dione precursor using flash vacuum pyrolytic CO extrusion, and by photochemical cycloreversions.^[27]

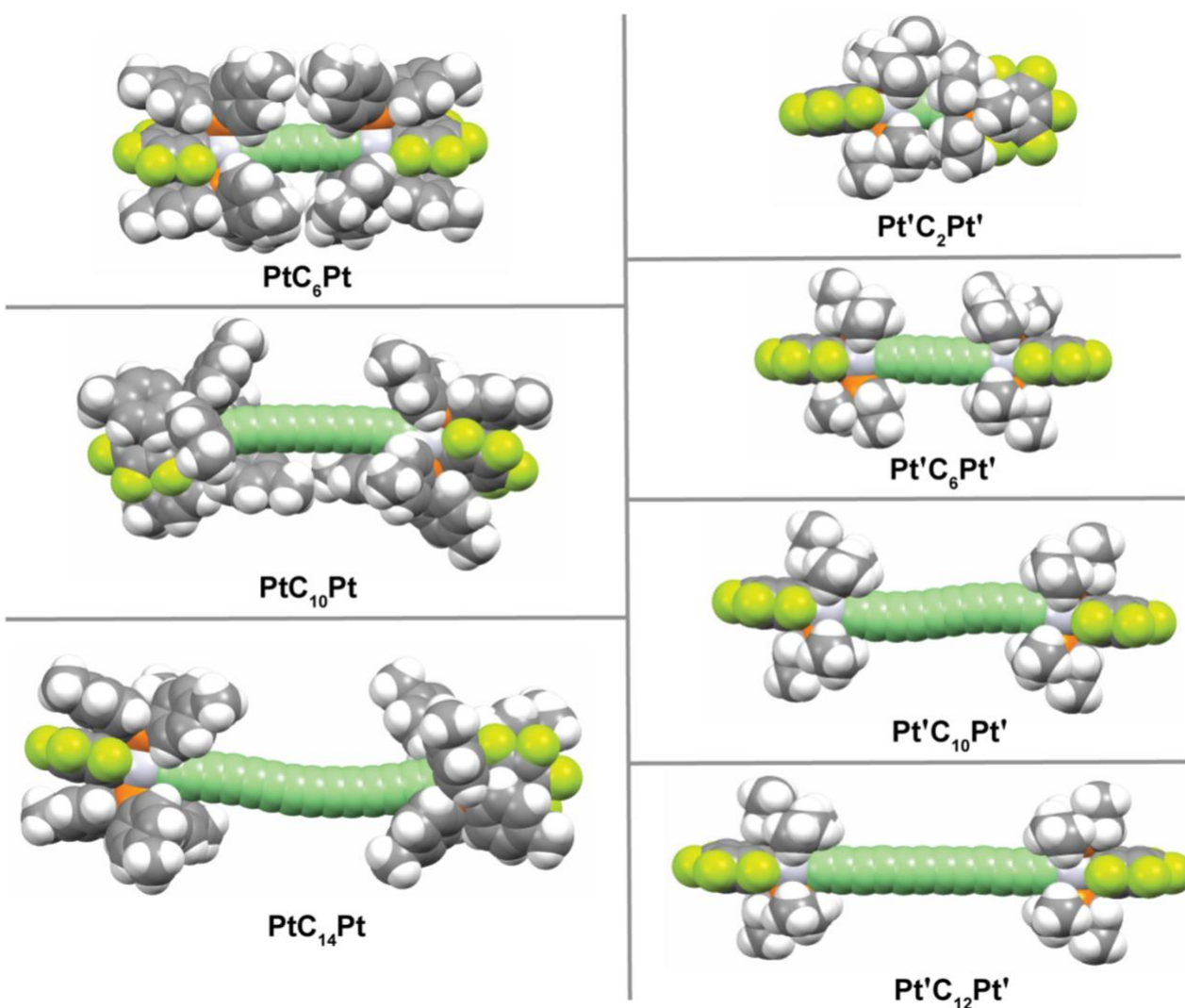


Figure 6. Space filling representations of crystallographically characterized diplatinum complexes.

Our crystallographic data fill in several "missing links" among structurally characterized diplatinum polyynediyl complexes. Computational results identify a variety of monotonic trends in the $L_yPtC_xPtL_y$ bond lengths as x is increased,^[28] one of particular importance being the degree of bond length alternation (BLA).^[4b,29] However, the experimental bond lengths have error bars, commonly expressed as esd values, and these are often greater than the differences between computed distances. In Table S3, the new data for **Pt'C₂Pt'** and **Pt'C₁₀Pt'** are interpolated into existing data for **Pt'C₆Pt'** and **Pt'C₁₂Pt'**. Unfortunately, statistically meaningful trends are challenging to discern.

Nonetheless, the crystal structures are very helpful in visualizing various steric properties. Figure 6 shows how the new complexes **PtC₁₀Pt** and **PtC₁₄Pt** allow improved access to the sp carbon chain relative to the previously reported **PtC₆Pt**. The (C≡C)₃ segment in the latter has proved remarkably unreactive in a variety of attempted additions and cyclotrimerizations, some of which have been documented with other polyynes.^[30] However, it has proved possible to prepare dicobalt adducts of the next higher homolog, **PtC₈Pt**.^[31]

Figure 6 also shows that the platinum endgroups of the PEt₃-substituted complexes **Pt'C₆Pt'** and **Pt'C₁₀Pt'** are much less bulky than those of **PtC₆Pt** and **PtC₁₀Pt**. This decrease presumably accounts for ready formation of **Pt'C₂Pt'** in Scheme 3, as opposed to the failure to realize **PtC₂Pt**. There are no van der Waals contacts between the endgroups in **Pt'C₂Pt'** (closest C-C distance = 3.65 Å), but there are conformational consequences. First, note that in **Pt'C₆Pt'**, **Pt'C₁₀Pt'**, and **Pt'C₁₂Pt'**, the C₆F₅ groups on opposite termini are coplanar. This can be quantified by the angle between the (P-Pt_a-P)⋯Pt_b and (P-Pt_b-P)⋯Pt_a planes, which is 0° in all three cases (Table S3). In contrast, in **Pt'C₂Pt'** the planes are nearly orthogonal (87.2°). This converts what would be eclipsing P-Pt-P units to staggered moieties with attenuated steric interactions.

This poses the question as to why the remote C₆F₅ groups in **Pt'C₆Pt'**, **Pt'C₁₀Pt'**, and **Pt'C₁₂Pt'** should be coplanar to begin with. DFT calculations indicate essentially no electronic barrier to rotation about the Pt⋯Pt axis.^[28] Hence, packing forces are likely at work. The same preference is also seen in the series **PtC_xPt**, although secondary conformational features^[32] such

as chain bending distort the plane/plane angles. Those for **PtC₁₀Pt** and **PtC₁₄Pt** are 61.9° and 69.6°. Finally, it should be emphasized that there are many other complexes with $L_yMC\equiv CM'L'_y$ linkages.^[33] In some cases, rotational barriers associated with bulky termini can be quantified.^[35]

Two reviewers were curious whether so-called "even/odd effects", phenomena that are well established in certain contexts,^[34] might be manifested in any of the physical properties of **PtC₆Pt/PtC₁₀Pt/PtC₁₄Pt/PtC₁₈Pt** versus **PtC₈Pt/PtC₁₂Pt/PtC₁₆Pt/PtC₂₀Pt**. There are none that we can discern in any of the spectroscopic properties. Furthermore, the computational studies cited above reveal only trends that are monotonic in C_x (HOMO or LUMO energies, UV/visible λ_{\max} , oscillator strengths, etc.).^[28]

To our knowledge, the ethynediyl extrusion reactions documented herein (Schemes 4 and s1) and by other research groups^[1,9a,19,20] have no precedent or counterpart in classical shorter-chain polyene chemistry. The mechanisms remain a mystery, especially as $\equiv C-C\equiv$ σ bonds commonly have the highest dissociation energies.^[36] An initial computational approach might involve a series of model intermediates $[X(C\equiv C)_n]^{z+}$, and defining the energetics of C_2 extrusion as a function of n and z (-1, 0, 1). Until there is more mechanistic insight, only empirical generalizations on avoiding these unwelcome side reactions will be possible.

In conclusion, this study has demonstrated the utility of Sonogashira-type heterocoupling reactions for expanding the availability of the title polyynes. This series of complexes has largely been restricted to even numbers of triple bonds due to the Hay oxidative homocoupling protocols commonly employed. Irrespective of endgroup, every polyene chain length that can be accessed aids in modeling the properties of the sp carbon allotrope, carbyne.^[3-5] Also, the detailed documentation of spontaneous ethynediyl extrusion in Hay heterocoupling protocols should assist future synthetic studies.

■ EXPERIMENTAL SECTION

All instrumentation and characterization protocols were identical to those in recent full papers in this series.^[3,9,20] These are summarized, together with chemical sourcing and purification, in the supporting information. All reactions were conducted under dry inert atmospheres us-

ing conventional Schlenk techniques, but workups were carried out in air.

***trans,trans*-[$(C_6F_5)(p\text{-tol}_3P)_2Pt(C\equiv C)_5Pt(Pp\text{-tol}_3)_2(C_6F_5)$] ($PtC_{10}Pt$).** A Schlenk flask was charged with $PtCl$ (0.047 g, 0.047 mmol),^[9a] Et_2NH (20 mL), CH_2Cl_2 (10 mL) and $CuCl$ (0.004 g, 0.038 mmol) with stirring. After the mixture became homogeneous it was cooled to -45 °C (dry ice/acetonitrile). Another Schlenk flask was charged with $PtC_{10}Si$ (0.051 g, 0.042 mmol)^[12] and CH_2Cl_2 (20 mL) and cooled to -45 °C. Then $n\text{-Bu}_4N^+ F^-$ (1.0 M in THF/5 wt% H_2O , 0.013 mL, 0.013 mmol) was added with stirring. TLC monitoring (silica gel, 1:7 v/v CH_2Cl_2 /hexanes) showed the complete conversion of $PtC_{10}Si$ to $PtC_{10}H$ over 15 min. The sample was transferred by cannula to the solution of $PtCl$, which was allowed to warm to room temperature. After 3 d, the solvent was removed by oil-pump vacuum. The residue was extracted with hexanes (30 mL) and toluene (10 mL). The extracts were passed in sequence through a neutral alumina column (2×20 cm, packed in hexanes). The solvent was removed from the toluene eluates by rotary evaporation. The residue was chromatographed on a silica gel column (3×20 cm, packed in hexanes, eluted with a 0:4 \rightarrow 1:4 v/v CH_2Cl_2 /hexanes gradient). The yellow band was taken to dryness by oil-pump vacuum to give $PtC_{10}Pt$ as a yellow powder (0.037 g, 0.018 mmol, 42%), which decomposed at 208 °C without melting (open capillary). Anal. Calcd. for $C_{106}H_{84}F_{10}P_4Pt_2$ (2061.83): C, 61.69; H, 4.07. Found: C, 61.77; H, 4.19.

NMR (δ /ppm, $CDCl_3$): 1H (500 MHz, cryoprobe) 7.45-7.41 (m, 24H, *o* to P),^[37] 7.03 (d, $^3J_{HH} = 10$ Hz, 24H, *m* to P),^[37] 2.29 (s, 36H, \underline{CH}_3); $^{13}C\{^1H\}$ (126 MHz, cryoprobe)^[38] 144.8 (dd, $^1J_{CF} = 226$ Hz, $^2J_{CF} = 28$ Hz, *o* to Pt), 139.8 (s, *p* to P), 136.7 (dm, $^1J_{CF} = 67$ Hz, *p* to Pt), 134.7 (dm, $^1J_{CF} = 74$ Hz, *m* to Pt), 133.2 (virtual t, $^2J_{CP} = 13$ Hz,^[39] *o* to P), 127.7 (virtual t, $^3J_{CP} = 11$ Hz,^[39] *m* to P), 126.1 (virtual t, $^1J_{CP} = 60$ Hz,^[39] *i* to P), 103.2 (br s, $PtC\equiv C$),^[38] 94.9 (s, $PtC\equiv C$), 63.8, 60.9, 56.7 (3 s, $PtC\equiv C(\underline{C}\equiv\underline{C})\underline{C}$), 20.3 (s, \underline{CH}_3); $^{31}P\{^1H\}$ (202 MHz) 17.2 (s, $^1J_{PPt} = 2588$ Hz).^[41] IR (powder film, cm^{-1}) 2132/2081/2037 (w/m/s, $\nu_{C\equiv C}$). UV-vis (nm, 2.25×10^{-6} M in CH_2Cl_2 , (ϵ , $M^{-1}cm^{-1}$)) 251 (77000), 282 (101000), 304 (123000), 346 (177000), 364 (281000), 390 (292000).

***trans,trans*-[$(C_6F_5)(p\text{-tol}_3P)_2Pt(C\equiv C)_7Pt(Pp\text{-tol}_3)_2(C_6F_5)$] ($PtC_{14}Pt$).** A Schlenk flask

was charged with **PtCl** (0.037 g, 0.037 mmol),^[9a] *t*-BuOK (0.034 g, 0.301 mmol), KPF₆ (0.056 g, 0.304 mmol), CuCl (0.0042 g, 0.041 mmol), THF (50 mL) and MeOH (10 mL). The mixture was vigorously stirred and cooled to –45 °C (dry ice/acetonitrile). Another Schlenk flask was charged with **PtC₁₄Si** (0.041 g, 0.032 mmol)^[12] and CH₂Cl₂ (20 mL) and cooled to –45 °C. Then *n*-Bu₄N⁺ F[–] (1.0 M in THF/5 wt% H₂O, 0.010 mL, 0.010 mmol) was added with stirring. TLC monitoring (silica gel, 1:7 v/v CH₂Cl₂/hexanes) showed the complete conversion of **PtC₁₄Si** to **PtC₁₄H** over 15 min. The sample was transferred via cannula to the solution of **PtCl**, which was allowed to warm to room temperature. After 3 d, a workup identical to that for **PtC₁₀Pt** gave **PtC₁₄Pt** as a dark yellow powder (0.028 g, 0.013 mmol, 41%), which decomposed at 224 °C without melting (open capillary). Anal. Calcd. for C₁₁₀H₈₄F₁₀P₄Pt₂ (2109.83): C, 62.56; H, 3.98. Found: C, 62.71; H, 3.94.

NMR (δ/ppm, CDCl₃): ¹H (500 MHz, cryoprobe) 7.45-7.41 (m, 24H, *o* to P),^[37] 7.11 (d, ³J_{HH} = 10 Hz, 24H, *m* to P),^[37] 2.35 (s, 36H, CH₃); ¹³C {¹H} (126 MHz, cryoprobe)^[38] 145.9 (dm, ¹J_{CF} = 231 Hz, *o* to Pt), 141.2 (s, *p* to P), 137.8 (dm, ¹J_{CF} = 69 Hz, *p* to Pt), 135.9 (dm, ¹J_{CF} = 76 Hz, *m* to Pt), 134.4 (virtual t, ²J_{CP} = 13 Hz,^[39] *o* to P), 128.9 (virtual t, ³J_{CP} = 12 Hz,^[39] *m* to P), 127.0 (virtual t, ¹J_{CP} = 60 Hz,^[39] *i* to P), 108.3 (br s, PtC≡C),^[38] 95.4 (s, PtC≡C), 66.5, 64.4, 62.3, 60.6, 57.1 (5 s, PtC≡C(C≡C)₂C), 21.5 (s, CH₃); ³¹P {¹H} (202 MHz) 17.4 (s, ¹J_{PtP} = 2613 Hz).^[41] IR (powder film, cm^{–1}) 2132/2081/2037 (w/m/s, ν_{C≡C}). UV-vis (nm, 2.25 × 10^{–6} M in CH₂Cl₂, (ε, M^{–1}cm^{–1})) 289 (113000), 286 (125000), 317 (142000), 312 (156000), 353 (224000), 374 (324000), 404 (327000).

trans,trans-[(C₆F₅)(*p*-tol₃P)₂Pt(C≡C)₉Pt(*Pp*-tol₃)₂(C₆F₅)] (PtC₁₈Pt). **PtCl** (0.050 g, 0.050 mmol),^[9a] *t*-BuOK (0.045 g, 0.40 mmol), KPF₆ (0.074 g, 0.40 mmol), CuCl (0.0047 g, 0.048 mmol), THF (50 mL), MeOH (10 mL), **PtC₁₈Si** (0.048 g, 0.041 mmol),^[12] CH₂Cl₂ (20 mL), and *n*-Bu₄N⁺ F[–] (1.0 M in THF/5 wt% H₂O, 0.012 mL, 0.012 mmol) were combined in a procedure analogous to that for **PtC₁₄Pt**. An identical workup gave **PtC₁₈Pt** as a dark yellow powder (0.028 g, 0.013 mmol, 32%), which decomposed at 198 °C without melting (open capillary). Anal. Calcd. for C₁₁₄H₈₄F₁₀P₄Pt₂ (2157.83): C, 63.39; H, 3.89. Found: C, 63.23; H, 4.03.

NMR (δ /ppm, CDCl_3): ^1H (500 MHz, cryoprobe) 7.45-7.41 (m, 24H, *o* to P),^[37] 7.11 (d, $^3J_{\text{HH}} = 10$ Hz, 24H, *m* to P),^[37] 2.36 (s, 36H, $\text{C}\underline{\text{H}}_3$); $^{13}\text{C}\{^1\text{H}\}$ (126 MHz, cryoprobe)^[38,42] 145.9 (dd, $^2J_{\text{CF}} = 26$ Hz, *o* to Pt), 141.2 (s, *p* to P), 137.8 (dm, $^1J_{\text{CF}} = 63$ Hz, *p* to Pt), 135.7 (dm, $^1J_{\text{CF}} = 88$ Hz, *m* to Pt), 134.3 (virtual t, $^2J_{\text{CP}} = 13$ Hz,^[39] *o* to P), 128.9 (virtual t, $^3J_{\text{CP}} = 11$ Hz,^[39] *m* to P), 126.9 (virtual t, $^1J_{\text{CP}} = 62$ Hz,^[39] *i* to P), 95.1 (s, $\text{PtC}\equiv\text{C}$), 67.3, 65.6, 64.0, 62.7, 61.4, 60.1, 56.9 (7 s, $\text{PtC}\equiv\text{C}(\underline{\text{C}}\equiv\text{C})_3$), 21.5 (s, $\underline{\text{C}}\text{H}_3$); $^{31}\text{P}\{^1\text{H}\}$ (202 MHz) 17.2 (s, $^1J_{\text{PPt}} = 2588$ Hz).^[41] IR (powder film, cm^{-1}) 2132/2081/2037 (w/m/s, $\nu_{\text{C}\equiv\text{C}}$). UV-vis (nm, 2.25×10^{-6} M in CH_2Cl_2 , (ϵ , $\text{M}^{-1}\text{cm}^{-1}$)) 293 (122000), 308 (128000), 324 (158000), 349 (223000), 371 (352000), 384 (326000), 417 (346000).

***trans,trans*-(C_6F_5)(Et_3P) $_2$ Pt($\text{C}\equiv\text{C}$) $_5$ Pt(PEt_3) $_2$ (C_6F_5) ($\text{Pt}'\text{C}_{10}\text{Pt}'$).** A Schlenk flask was charged with $\text{Pt}'\text{C}_{10}\text{Pt}$ (0.056 g, 0.027 mmol) and CH_2Cl_2 (30 mL). Then PEt_3 (0.018 mL, 0.124 mmol) was added with stirring. After 16 h, the solvent was removed by oil pump vacuum. Ethanol (10 mL) was added to the oily residue, which was kept at 4 °C. After 2 h, the solid was collected by filtration, washed with ethanol (2×10 mL), and dried by oil-pump vacuum to give $\text{Pt}'\text{C}_{10}\text{Pt}'$ as a yellow powder (0.028 g, 0.021 mmol, 78%), which decomposed at 196 °C without melting (open capillary). Anal. Calcd. for $\text{C}_{46}\text{H}_{60}\text{F}_{10}\text{P}_4\text{Pt}_2$ (1316.28): C, 41.94; H, 4.56. Found: C, 41.89; H, 4.59.

NMR (δ /ppm, CDCl_3): ^1H (500 MHz, cryoprobe) 1.74 (m, 24H, $\text{C}\underline{\text{H}}_2$), 1.07 (m, 36H, $\text{C}\underline{\text{H}}_3$); $^{13}\text{C}\{^1\text{H}\}$ (126 MHz, cryoprobe) 147.0 (dd, $^1J_{\text{CF}} = 224$ Hz, $^2J_{\text{CF}} = 19$ Hz, *o* to Pt), 137.1 (dm, $^1J_{\text{CF}} = 244$ Hz, *m/p* to Pt), 119.1 (m, $^1J_{\text{CPt}} = 679$ Hz,^[41] $^2J_{\text{CP}} = 111$ Hz, *i* to Pt), 106.3 (br s, $^1J_{\text{CPt}} = 1033$ Hz,^[41] $\text{Pt}\underline{\text{C}}\equiv\text{C}$), 90.9 (s, $^2J_{\text{CPt}} = 282$ Hz,^[41] $\text{PtC}\equiv\text{C}$), 64.9, 62.1, 57.4 (3 s, $\text{PtC}\equiv\text{C}(\underline{\text{C}}\equiv\text{C})$), 15.9 (virtual t, $^1J_{\text{CP}} = 35$ Hz,^[39] $\underline{\text{C}}\text{H}_2$), 7.9 (s, $\underline{\text{C}}\text{H}_3$); $^{31}\text{P}\{^1\text{H}\}$ (202 MHz) 12.8 (s, $^1J_{\text{PPt}} = 2380$ Hz).^[41] IR (powder film, cm^{-1}) 2132/2081/2037 (w/m/s, $\nu_{\text{C}\equiv\text{C}}$). UV-vis (nm, 2.42×10^{-6} M in CH_2Cl_2 , (ϵ , $\text{M}^{-1}\text{cm}^{-1}$)) 283 (44000), 316 (51300), 348 (161000).

***trans,trans*-(C_6F_5)(Et_3P) $_2$ Pt $\text{C}\equiv\text{C}$ Pt(PEt_3) $_2$ (C_6F_5) ($\text{Pt}'\text{C}_2\text{Pt}'$).** A Schlenk flask was charged with $\text{Pt}'\text{C}_2\text{H}$ (0.162 g, 0.260 mmol),^[16] $\text{Pt}'\text{Cl}$ (0.165 g, 0.260 mmol),^[16] *t*-BuOK (0.035 g, 0.31 mmol), KPF_6 (0.058 g, 0.316 mmol), CuCl (0.0049 g, 0.049 mmol), THF (20 mL), and MeOH

(20 mL) with stirring. Over the course of 2 d, TLC monitoring (silica gel, 1:3 v/v CH₂Cl₂/hexanes) showed the consumption of **Pt'C₂H** and **Pt'Cl** (R_f 0.65, 0.15) and the appearance of a product (R_f 0.50). The solvent was removed by oil-pump vacuum. The residue was extracted with CH₂Cl₂ and filtered through a short Celite pad. The solvent was removed by rotary evaporation and the residue chromatographed (30 × 2 cm column, silica gel packed in hexanes, eluted with a 0:4 → 1:4 v/v CH₂Cl₂/hexanes gradient). The solvent was removed from the product containing fractions by oil-pump vacuum to give **Pt'C₂Pt'** as a white solid (0.216 g, 0.177 mmol, 68%), which started to blacken at 135 °C and melted at 146 °C (open capillary). Anal. Calcd. for C₃₈H₆₀F₁₀P₄Pt₂ (1220.92): C, 37.37; H, 4.92. Found: C, 37.27; H, 4.78.

NMR (δ /ppm, CDCl₃): ¹H (500 MHz, cryoprobe) 1.78 (m, 24H, CH₂), 1.05 (m, 36H, CH₃); ¹³C{¹H} (126 MHz, cryoprobe) 147.2 (dd, ¹J_{CF} = 244 Hz, ²J_{CF} = 21 Hz, *o* to Pt), 136.7 (dm, ¹J_{CF} = 248 Hz, *m/p* to Pt), 122.7 (t, ²J_{CF} = 59 Hz, *i* to Pt), 116.4 (t, ²J_{CP} = 21 Hz, ^[41] Pt≡C), 15.4 (virtual t, ¹J_{CP} = 17.0 Hz, ^[39] ²J_{CPt} = 33 Hz, ^[41] CH₂), 8.0 (s, ³J_{CPt} = 24 Hz, ^[41] CH₃); ³¹P{¹H} (202 MHz) 14.8 (s, ¹J_{Pt} = 2483 Hz). ^[41] IR (powder film, cm⁻¹) 2114 (m, $\nu_{C\equiv C}$).

Reaction of PtC₁₀Si and HC₄Si in Scheme 4. A three-neck round bottom flask was fitted with a gas dispersion tube, charged with **PtC₁₀Si** (0.427 g, 0.354 mmol)^[12] and THF (50 mL), and cooled to -78 °C. A Schlenk flask was charged with CuCl (0.139 g, 1.41 mmol), acetone (20 mL), and TMEDA (0.266 mL, 0.206 g, 1.77 mmol) with stirring (rt, 0.5 h), after which a green solid separated from a blue supernatant. Then wet *n*-Bu₄N⁺ F⁻ (1.0 M in THF, 5 wt% water, 0.10 mL, 0.10 mmol) was added to the three-neck flask with stirring. After 5 min (silica gel TLC, 1:9 v/v ethyl acetate/hexanes, showed no remaining educt), Me₃SiCl (0.12 mL, 0.94 mmol), cold acetone (-45 °C, 70 mL), and **HC₄Si** (1.307 g, 7.954 mmol)^[12] were sequentially added. Then oxygen was bubbled through the tube and the blue supernatant (rt) added with stirring. After 1 h, the bath was removed and hexanes (140 mL) added. The dark green suspension was filtered through a pad of silica gel (2.5 × 10 cm, packed in 1:1 v/v acetone/hexanes), which was rinsed (1:1 v/v acetone/hexanes) until the filtrate became colorless. The solvents were removed from the filtrate by rotary evaporation at 20 °C and the red brown residue chromatographed on a silica gel column (3.5 × 30

cm, packed in hexanes, eluted first with hexanes then with a CH₂Cl₂ gradient until 3:1 v/v CH₂Cl₂/hexanes). The solvents were removed from the product containing fractions by rotary evaporation and oil pump vacuum to give an inseparable 23:77 mixture (assayed from Figure 5) of **PtC₁₂Si** and **PtC₁₄Si** as orange-brown solid (0.191 g, 0.152 mmol, 43%).^[22]

NMR δ /ppm, CDCl₃, sp, sp³ and phosphorus signals only, **PtC₁₄Si/PtC₁₂Si**: ¹H (500 MHz) 2.4 (1 × s, 18H, CH₃, *p* to P), 0.99/0.98 (2 × t, ³J_{HH} = 7.9 Hz, 9H, SiCH₂CH₃), 0.64/0.63 (2 × q, ³J_{HH} = 7.9 Hz, 6H, SiCH₂); ¹³C{¹H} (126 MHz)^[38] 109.9/109.2 (2 × br s, PtC≡C),^[40] 94.8 (1 × s, PtC≡C), 88.9/89.2 (2 × s, C≡CSi), 86.78/85.97 (2 × s, C≡CSi), 67.2/66.9, 65.6/65.3, 64.2/63.9, 63.3/62.5, 62.1/-, 61.8/-, 61.5/61.2, 60.62/60.59, 59.59/59.55, 56.5/- (remaining C≡), 21.3 (1 × s, CH₃), 7.3 (1 × s, SiCH₂CH₃), 4.0/4.1 (2 × s, SiCH₂); ³¹P{¹H} (202 MHz) 18.03 (1 × s, ¹J_{Pt} = 2608 Hz).^[41]

Crystallography. The following structure solution is representative, and others are detailed in the SI. A CHCl₃ solution of **PtC₁₀Pt** was layered with hexanes and kept at 4 °C. After 3 d, orange plates were collected. Cell parameters were determined from 45 data frames taken at widths of 1° and refined with 11365 reflections using APEX3.^[43] Data were corrected for Lorentz and polarization factors, and (using SADABS)^[44] crystal decay and absorption effects. Systematic reflection conditions and statistical tests suggested the space group *C2/c*, which was confirmed by SHELXT.^[44] Two molecules of chloroform were found per **PtC₁₀Pt** molecule. Hydrogen atom positions were calculated and refined using a riding model. All non-hydrogen atoms were refined anisotropically. The absence of additional symmetry and voids was confirmed using PLATON (ADDSYM).^[45] The structure was refined (weighted least squares refinement on *F*²) to convergence.^[44,46]

Supporting Information

Additional syntheses, and NMR, mass spectrometric, and crystallographic data are available in the Supporting Information of this article. Additional references are cited within the Supporting Information.

CCDC 2353153-2353155, and 2354444 contain the supplementary crystallographic data for this paper. These data can be obtained free of charge via www.ccdc.cam.ac.uk/data_request/cif, or by emailing data_request@ccdc.cam.ac.uk, or by contacting The Cambridge Crystallographic Data Centre, 12 Union Road, Cambridge CB2 1EZ, UK; fax: +44 1223 336033.

Acknowledgements

The US National Science Foundation (NSF; CHE-1566601, CHE-1900549) and Welch Foundation (A-2189) are thanked for support.

Conflict of Interests

The authors declare no conflict of interest.

Data Availability Statement

The data that support the findings of this study are available in the main text and supplementary material of this article.

Keywords: platinum, polyynyl complexes, Sonogashira coupling, Hay coupling, crystal structures

ORCID

John A. Gladysz: 0000-0002-7012-4872

Sourajit Dey Baksi: 0000-0002-0455-1817

■ REFERENCES (All titles are given in the capitalization format of the original article)

[1] a) Chalifoux, W. A.; Tykwinski, R. R. Synthesis of polyynes to model the *sp*-carbon allotrope carbyne. *Nature Chem.* **2010**, *2*, 967-971. b) Gao, Y.; Hou, Y.; Gárnez, F. G.; Ferguson, M. J.; Casado, J.; Tykwinski, R. R. The loss of endgroup effects in long pyridyl-encapped oligoynes on the way to carbyne. *Nature Chem.* **2020**, *12*, 1143-1149.

[2] Patrick, C. W.; Gao, Y.; Gupta, P.; Thompson, A. L.; Parker, A. W.; Anderson, H. L. Masked alkynes for synthesis of threaded carbon chains. *Nature Chem.* **2024**, *16*, 193-200.

[3] Arora, A.; Dey Baksi, S.; Weisbach, N.; Amini, H. Bhuvanesh, N.; Gladysz, J. A. Monodisperse Molecular Models for the *sp* Carbon Allotrope Carbyne; Syntheses, Structures, and Properties of Diplatinum Polyynediyl Complexes with PtC₂₀Pt to PtC₅₂Pt Linkages. *ACS Cent. Sci.* **2023**, *9*, 2225-2240.

[4] Overviews of synthetic milestones: a) Chalifoux, W. A.; Tykwinski, R. R. Synthesis of extended polyynes: Toward carbyne. *Comptes Rendus Chimie* **2009**, *12*, 341-358. b) Gao, Y.; Tykwinski, R. R. Advances in Polyynes to Model Carbyne. *Acc. Chem. Res.* **2022**, *55*, 3616-3630.

[5] a) Lv, C.-F.; Yang, X.-G.; Shan, C.-X. One-dimensional *sp* carbon: Synthesis, properties, and modifications. *Chin. Phys. B* **2022**, *31*, 128103. b) Pan, B.; Xiao, J.; Li, J.; Liu, Pu.; Wang, C.; Yang, G. Carbyne with finite length: The one-dimensional *sp* carbon. *Sci. Adv.* **2015**, *1*, e1500857.

[6] a) Heimann, R. B.; Evsyukov, S. E.; Koga, Y. Carbon Allotropes: A Suggested Classification Scheme Based on Valence Orbital Hybridization. *Carbon* **1997**, *35*, 1654-1658. b) Georgakilas, V.; Perman, J. A.; Tucek, J.; Zboril, R. Broad Family of Carbon Nanoallotropes: Classification, Chemistry, and Applications of Fullerenes, Carbon Dots, Nanotubes, Graphene, Nanodiamonds, and Combined Superstructures. *Chem. Rev.* **2015**, *115*, 4744-4822.

[7] Extance, A. Carbon's allotrope explosion. *Chemistry World* **2024**, April, pp 32-33.

[8] a) Diederich, F.; Rubin, Y.; Chapman, O. L.; Goroff, N. S. Synthetic Routes to the Cyclo[n]carbons. *Helv. Chim. Acta* **1994**, *77*, 1441-1457. b) Sale, A. C.; Murray, A. H.; Prenzel, D.; Hampel, F.; Luca, L. D.; Tykwinski, R. R. Diels–Alder Cycloaddition of Tetraphenylcyclopentadienone and 1,3,5-Hexatriynes. *Eur. J. Org. Chem.* **2016**, 2274-2283.

[9] a) Mohr, W.; Stahl, J.; Hampel, F.; Gladysz, J. A. Synthesis, Structure, and Reactivity of sp Carbon Chains with Bis(phosphine)Pentafluorophenylplatinum Endgroups: Butadiynediyl (C_4) through Hexadecaoctaynediyl (C_{16}) Bridges, and Beyond. *Chem. Eur. J.* **2003**, *9*, 3324-3340. b) Weisbach, N.; Kuhn, H.; Amini, H.; Ehnbohm, A.; Hampel, F.; Reibenspies, J. H.; Hall, M. B.; Gladysz, J. A. Triisopropylsilyl (TIPS) Alkynes as Building Blocks for Syntheses of Platinum Triisopropylsilylpolyyne and Diplatinum Polyynediyl Complexes. *Organometallics* **2019**, *38*, 3294-3310. c) Amini, H.; Baranová, Z.; Weisbach, N.; Gauthier, S.; Bhuvanesh, N.; Reibenspies, J. H.; Gladysz, J. A. Syntheses, Structures, and Spectroscopic Properties of 1,10-Phenanthroline-Based Macrocycles Threaded by PtC_8Pt , $PtC_{12}Pt$, and $PtC_{16}Pt$ Axles: Metal-Capped Rotaxanes as Insulated Molecular Wires. *Chem. Eur. J.* **2019**, *25*, 15896-15914.

[10] Owen, G. R.; Stahl, J.; Hampel, F.; Gladysz, J. A. Coordination-Driven Self-Assembly, Structures, and Dynamic Properties of Diplatinum Hexatriynediyl and Butadiynediyl Complexes in which the sp Carbon Chains are Shielded by sp^3 Carbon Chains: Towards Endgroup-Endgroup Interactions. *Chem. Eur. J.* **2008**, *14*, 73-87.

[11] a) Chinchilla, R.; Nájera, C. Recent advances in Sonogashira reactions. *Chem. Soc. Rev.* **2011**, *40*, 5084-5121. b) Sonogashira, K.; Yatake, T.; Tohda, Y.; Takahashi, S.; Hagihara, N. Novel Preparation of σ -Alkynyl Complexes of Transition Metals by Copper(I) Iodide-catalysed Dehydrohalogenation. *J. Chem. Soc., Chem. Commun.* **1977**, 291-292. c) Sonogashira, K.; Takahashi, S.; Hagihara, N. A New Extended Chain Polymer. Poly[*trans*-bis(tri-*n*-butylphosphine)platinum 1,4-butadiynediyl]. *Macromolecules* **1977**, *10*, 879-880.

[12] Amini, H.; Weisbach, N.; Gauthier, S.; Kuhn, H.; Bhuvanesh, N.; Hampel, F.; Reibenspies, J. H.; Gladysz, J. A. Trapping of Terminal Platinapolyynes by Copper(I) Catalyzed Click Cycloadditions; Probes of Labile Intermediates in Syntheses of Complexes with Extended sp Carbon Chains, and Crystallographic Studies. *Chem. Eur. J.* **2021**, *27*, 12619-12634.

[13] Without CuCl: a) Coat, F.; Guillemot, M.; Paul, F.; Lapinte, C. First Synthesis and Spectroscopic Characterization of Isolated Butatrienyliene Complexes of Transition Metals. *J. Organomet. Chem.* **1999**, *578*, 76-84. b) Coat, F.; Guillevic, M.-A.; Toupet, L.; Paul, F.; Lapinte, C. Elemental Carbon Chain Bridging Two Iron Centers: Syntheses and Spectroscopic Properties

of Donor–Acceptor [Fe]–C₄–[Fe] Complexes Isolated in Two Different Oxidation States. X-ray Crystal Structure of [Cp*(dppe)Fe–C₄–Fe(CO)₂Cp*]. *Organometallics* **1997**, *16*, 5988–5998. c) Paul, F.; Meyer, W. E.; Toupet, L.; Jiao, H.; Gladysz, J. A.; Lapinte, C. A "Conjugal" Consanguineous Family of Butadiynediyl-Derived Complexes: Synthesis and Electronic Ground States of Neutral, Radical Cationic, and Dicationic Iron/Rhenium C₄ Species. *J. Am. Chem. Soc.* **2000**, *122*, 9405–9414.

[14] With CuCl: de Quadras, L.; Shelton, A. H.; Kuhn, H.; Hampel, F.; Schanze, K. S.; Gladysz, J. A. Syntheses, Structures, and Electronic and Photophysical Properties of Unsymmetrically Substituted Butadiynediyl and Hexatriynediyl Complexes Derived from (C₆F₅)(R₃P)₂Pt, (*p*-tol)(R₃P)₂Pt, and (Ph₃P)Au End-Groups *Organometallics* **2008**, *27*, 4979–4991.

[15] Zhang, T.; Bhuvanesh, N.; Gladysz, J. A. A Quest for Atropisomerism in Cojoined Square-Planar Metal Complexes: Syntheses and Structures of Sterically Congested Diplatinum Ethynediyl Adducts. *Eur. J. Inorg. Chem.* **2017**, *2017*, 1017–1025.

[16] Stahl, J.; Bohling, J. C.; Peters, T. B.; de Quadras, L.; Gladysz, J. A. En route to diplatinum polyynediyl complexes *trans,trans*-(Ar)(R₃P)₂Pt(C≡C)_{*n*}Pt(PR₃)₂(Ar): Untold tales, including end-group strategies. *Pure Appl. Chem.* **2008**, *80*, 459–474.

[17] Mahanta, H.; Baishya, D.; Ahamed, Sk. S.; Paul, A. K. Chemical Dynamics Simulations on Association and Ensuing Dissociation of a Benzene–Hexafluorobenzene Molecular System. *J. Phys. Chem. A* **2019**, *123*, 5019–5026 and references cited therein.

[18] Zheng, Q.; Bohling, J. C.; Peters, T. B.; Frisch, A. C.; Hampel, F.; Gladysz, J. A. A Synthetic Breakthrough into an Unanticipated Stability Regime: A Series of Isolable Complexes in which C₆, C₈, C₁₀, C₁₂, C₁₆, C₂₀, C₂₄, and C₂₈ Polyynediyl Chains Span Two Platinum Atoms. *Chem. Eur. J.* **2006**, *12*, 6486–6505.

[19] a) Gibtner, T.; Hampel, F.; Gisselbrecht, J.-P.; Hirsch, A. End-Cap Stabilized Oligoynes: Model Compounds for the Linear sp Carbon Allotrope Carbyne. *Chem. Eur. J.* **2002**, *8*, 408–432. b) Eisler, S.; Slepko, A. D.; Elliott, E.; Luu, T.; McDonald, R.; Hegmann, F. A.; Tykwinski, R. R. Polyynes as a Model for Carbyne: Synthesis, Physical Properties, and Nonlinear Optical Response. *J. Am. Chem. Soc.* **2005**, *127*, 2666–2676. In this study, lowering the temperature of the

homocoupling suppressed C₂ loss. c) Chalifoux, W. A.; McDonald, R.; Ferguson, M. J.; Tykwinski, R. R. *tert*-Butyl-End-Capped Polyynes: Crystallographic Evidence of Reduced Bond-Length Alternation. *Angew. Chem., Int. Ed.* **2009**, *48*, 7915-7919; Polyine mit *tert*-Butyl-Endgruppen: kristallographischer Nachweis einer reduzierten Bindungslängenalternanz. *Angew. Chem.* **2009**, *121*, 8056-8060. d) Chalifoux, W. A.; Ferguson, M. J.; McDonald, R.; Melin, F.; Echegoyen, L.; Tykwinski, R. R. Adamantyl-encapped polyynes. *J. Phys. Org. Chem.* **2012**, *25*, 69-76.

[20] For byproducts derived from the loss of octatetraenediyl (C₈) fragments, see Dey Baksi, S.; Aggrey, J. O.; Bhuvanesh, N.; Gladysz, J. A. Reactions of Platinum Terminal Polyyne Complexes *trans*-(C₆F₅)(*p*-tol₃P)₂Pt(C≡C)_{*n*}H (*n* = 2–4) and *n*-BuLi, Generation of Functional Equivalents of Pt(C≡C)_{*n*}Li Species, and Derivatization with Organic and Inorganic Electrophiles. *Organometallics* **2024**, *43*, 1041-1050.

[21] Hay, A. S. Oxidative Couplings of Acetylenes. II. *J. Org. Chem.* **1962**, *27*, 3320-3321.

[22] The total yields are derived from the combined product masses, fitted to the mol ratios determined by NMR.

[23] As evidenced by non-Gaussian peaks, partial separations were sometimes achieved. Thus, special techniques (e.g., recycle HPLC) could potentially allow baseline separations. The baseline separation of the diplatinum complexes **PtC₁₆Pt**, **PtC₂₀Pt**, and **PtC₂₄Pt** (which differ by four sp carbon atoms) by analytical HPLC is possible.^[9a]

[24] Among other examples, this trend is evident for the Hay cross coupling of **PtC₈Si** and **HC₂Si** in reference [9a] (see bold header in that experimental section) and that of **PtC₈Si** and **HC₄Si** in reference [12].

[25] Jahnke, E.; Tykwinski, R. R. The Fritsch–Buttenberg–Wiechell rearrangement: Modern Applications for an Old Reaction. *Chem. Commun.*, **2010**, *46*, 3235-3249.

[26] a) DeCicco, R. C.; Black, A.; Li, L.; Goroff, N. S. An Iterative Method for the Synthesis of Symmetric Polyynes. *Eur. J. Org. Chem.* **2012**, 4699-4704. b) Štefko, M.; Tzirakis, M. D.; Breiten, B.; Ebert, M.-O.; Dumele, O.; Schweizer, W. B.; Gisselbrecht, J.-P.; Boudon, C.; Beels, M. T.; Biaggio, I.; Diederich, F. Donor–Acceptor (D–A)-Substituted Polyene Chromophores: Modulation of Their Optoelectronic Properties by Varying the Length of the Acetylene Spacer.

Chem. Eur. J. **2013**, *19*, 12693-12704. c) Klinger, C.; Vostrowsky, O.; Hirsch, A. Synthesis of Alkylene-Bridged Diphenyl-Oligoynes. *Eur. J. Org. Chem.* **2006**, 1508-1524. d) Bruce, M. I.; Cole, M. L.; Ellis, B. G.; Gaudio, M.; Nicholson, B. K.; Parker, C. R.; Skelton, B. W.; White, A. H. The series of carbon-chain complexes $\{\text{Ru}(\text{dppe})\text{Cp}^*\}_2\{\mu\text{-(C}\equiv\text{C)}_x\}$ ($x = 4-8, 11$): Synthesis, structures, properties and some reactions. *Polyhedron* **2015**, *86*, 43-56. e) See also Milan, D. C.; Al-Owaedi, O. A.; Oerthel, M.-C.; Marqués-González, S.; Brooke, R. J.; Bryce, M. R.; Cea, P.; Ferrer, J.; Higgins, S. J.; Lambert, C. J.; Low, P. J.; Manrique, D. Z.; Martin, S.; Nichols, R. J.; Schwarzacher, W.; García-Suárez, V. M. Solvent Dependence of the Single Molecule Conductance of Oligoyne-Based Molecular Wires. *J. Phys. Chem. C* **2016**, *120*, 15666-15674.

[27] a) Rubin, Y.; Lin, S. S.; Knobler, C. B.; Anthony, J.; Boldi, A. M.; Diederich, F. Solution-Spray Flash Vacuum Pyrolysis: A New Method for the Synthesis of Linear Polyynes with Odd Numbers of C \equiv C Bonds from Substituted 3,4-Dialkynyl-3-cyclobutene-1,2-diones. *J. Am. Chem. Soc.* **1991**, *113*, 6943-6949. b) Tobe, Y.; Umeda, R.; Iwasa, N.; Sonoda, M. Expanded Radialenes with Bicyclo[4.3.1]deca-1,2,3,4,5,6,7,8-octaene Units: New Precursors to Cyclo[n]carbons. *Chem. Eur. J.* **2003**, *9*, 5549-5559.

[28] Zhuravlev, F.; Gladysz, J. A. Electronic Structure and Chain-Length Effects in Diplatinum Polyynediyl Complexes *trans,trans*-[(X)(R₃P)₂Pt(C \equiv C)_nPt(PR₃)₂(X)]: A Computational Investigation. *Chem. Eur. J.* **2004**, *10*, 6510-6522.

[29] Giesecking, R. L.; Risko, C.; Brédas, J.-L. Distinguishing the Effects of Bond-Length Alternation versus Bond-Order Alternation on the Nonlinear Optical Properties of π -Conjugated Chromophores. *J. Phys. Chem. Lett.* **2015**, *6*, 2158-2162.

[30] Pigulski, B.; Gulia, N.; Szafert, S. Reactivity of Polyynes: Complex Molecules from Simple Carbon Rods. *Eur. J. Org. Chem.* **2019**, 1420-1445.

[31] Kuhn, H.; Hampel, F.; Gladysz, J. A. Syntheses, Structures, and Dynamic Properties of Dicobalt π Complexes of Diplatinum Polyynediyl Complexes. *Organometallics* **2009**, *28*, 4979-4987.

[32] Szafert, S.; Gladysz, J. A. Carbon In One Dimension: Structural Analysis of the Higher Conjugated Polyynes. *Chem. Rev.* **2003**, *103*, 4175-4205; Szafert, S.; Gladysz, J. A. Update 1 of:

Carbon In One Dimension: Structural Analysis of the Higher Conjugated Polyynes. *Chem. Rev.* **2006**, *106*, PR1-PR33.

[33] a) Griffith, C. S.; Koutsantonis, G. A. The Chemistry of Transition Metal Ethyne-1,2-diyl Complexes. *Aust. J. Chem.* **2012**, *65*, 698-722. b) Yu, C.-H.; Yang, X.; Ji, X.; Wang, C.-H.; Lai, Q.; Bhuvanesh, N.; Ozerov, O. V. Redox Communication between Two Diarylamido/Bis-(phosphine) (PNP)M Moieties Bridged by Ynediyl Linkers (M = Ni, Pd, Pt). *Inorg. Chem.* **2020**, *59*, 10153-10162. The authors regret the omission of this citation, which describes several Pt-(C≡C)_nLi species, from their related work in reference [20].

[34] a) Mishra, M. K.; Varughese, S.; Ramamurty, U.; Desiraju, G. R. Odd-Even Effect in the Elastic Moduli of α,ω -Alkanedicarboxylic Acids. *J. Am. Chem. Soc.* **2013**, *135*, 8121-8124. b) Yang, K.; Cai, Z.; Jaiswal, A.; Tyagi, M.; Moore, J. S.; Zhang, Y. Dynamic Odd–Even Effect in Liquid *n*-Alkanes near Their Melting Points. *Angew. Chem., Int. Ed.* **2016**, *55*, 14090-14095; Dynamic Odd–Even Effect in Liquid *n*-Alkanes near Their Melting Points. *Angew. Chem.* **2016**, *128*, 14296–1430. c) Dhiman, I.; Berg, M. C.; Petridis, L.; Smith, J. C.; Gautam, S. Dynamic odd–even effect in *n*-alkane systems: a molecular dynamics study. *Phys. Chem. Chem. Phys.* **2022**, *24*, 28403-28410.

[35] Weng, W.; Bartik, T.; Brady, M.; Bartik, B.; Ramsden, J. A.; Arif, A. M.; Gladysz, J. A. Synthesis, Structure, and Redox Chemistry of Heteropolymetallic Carbon Complexes with MC₂M', MC₄M', and MC₄M'C₄M Linkages. Transmetalations of Lithiocarbon Complexes (η^5 -C₅Me₅)Re(NO)(PPh₃)(C≡CLi) and (η^5 -C₅Me₅)Re(NO)(PPh₃)(C≡CC≡CLi). *J. Am. Chem. Soc.* **1995**, *117*, 11922-11931.

[36] Zavitsas, A. A. The Relation between Bond Lengths and Dissociation Energies of Carbon-Carbon Bonds. *J. Phys. Chem. A* **2003**, *107*, 897-898.

[37] The aryl ¹H NMR signal that appears as a doublet is assigned to the *meta* CH moiety, and that that appears as a multiplet (presumably due to stronger ³¹P coupling) is assigned to the *ortho* CH moiety.

[38] The *ipso* C₆F₅ signal was not observed.

[39] Hersh W. H. False AA'X Spin-Spin Coupling Systems in ¹³C NMR: Examples Invol-

ving Phosphorus and a 20-Year-Old Mystery in Off-Resonance Decoupling. *J. Chem. Educ.* **1997**, *74*, 1485-1488. The J values represent the distance between adjacent peaks in the apparent triplet.

[40] The expected first order couplings were not resolved due to poor signal/noise ratio.

[41] This coupling represents a satellite (d; $^{195}\text{Pt} = 33.8\%$) and is not reflected in the peak multiplicity given.

[42] The $\text{Pt}\underline{\text{C}}\equiv$ signal was not observed.

[43] *APEX3, Program for Data Collection on Area Detectors*. Bruker AXS Inc., Madison, WI 53711-5373 USA.

[44] a) Sheldrick, G. M. *SADABS, Program for Absorption Correction for Data from Area Detector Frames*. Bruker AXS Inc., Madison, WI 53711-5373 USA. b) Sheldrick, G. M. *SHELXT – Integrated space-group and crystal structure determination*. *Acta Cryst.* **2015**, *A71*, 3-8. c) Sheldrick, G. M. *Crystal structure refinement with SHELXL*. *Acta Cryst.* **2015**, *C71*, 3-8.

[45] Spek, A. L. *Single-crystal structure validation with the program PLATON*. *J. Appl. Cryst.* **2003**, *36*, 7-13.

[46] Dolomanov, O. V.; Bourhis, L. J.; Gildea, R. J.; Howard, J. A. K.; Puschmann, H. *OLEX2: A Complete Structure Solution, Refinement and Analysis Program*. *J. Appl. Cryst.* **2009**, *42*, 339-341.

